

Electron work function decrease in SIMS analysis induced by neutral cesium deposition

P. Philipp^{a,*}, T. Wirtz^a, H.-N. Migeon^a, H. Scherrer^b

^a *Département Science et Analyse des Matériaux (SAM), Centre de Recherche Public-Gabriel Lippmann, 41 rue du Brill, Belvaux L-4422, Luxembourg*

^b *Laboratoire de Physique des Matériaux, Ecole des Mines, Parc de Saurupt, Nancy Cedex F-54042, France*

Received 22 January 2007; received in revised form 23 March 2007; accepted 26 March 2007

Available online 4 April 2007

Abstract

The negative secondary ion yields in secondary ion mass spectrometry (SIMS) increase when electropositive elements, especially alkali metals, are used as primary ions. In previous papers by the same authors, useful yield variations of several elements have been studied experimentally with respect to the neutral cesium deposition conditions. Besides, the Cs surface concentrations have been simulated using the TRIDYN code. The determined secondary ion sensitivities have been discussed with respect to the experimental conditions and they have been compared to the electron-tunneling model describing ion emission from metallic and semi-conducting samples. In this paper, the variations of the electron work function of the sample will be studied with respect to the experimental conditions used in the previous papers. The energy distributions of negative secondary ions will be recorded for the different experimental conditions. The electron work function shift, on which is based the electron-tunneling model and which thus gives evidence for the influence of cesium on ion emission, is extracted from these distributions. The variations of the electron work function are discussed with respect to the experimental conditions as well as the simulated cesium surface concentration. Besides, the secondary ion sensitivities are plotted with respect to the electron work function, giving a direct comparison with the electron-tunneling model.

© 2007 Elsevier B.V. All rights reserved.

Keywords: Neutral Cs deposition; Electron work function variation; Useful yield; Secondary ion mass spectrometry; CMS

1. Introduction

Secondary ion mass spectrometry (SIMS) constitutes an extremely powerful technique for analyzing surfaces and thin films, which is in particular due to its excellent sensitivity, its high dynamic range and its good depth resolution [1,2]. It is widely used for the analysis of trace elements in solid materials like semi-conductors and thin films [1–3]. Emerging fields of applications for SIMS are biology and medicine in particular [4–6].

At the same time, the SIMS technique is hampered by the lack of quantification [7]: the ionization probability of secondary ions and thus the sensitivity of the analysis depends on the sample composition. This phenomenon is known as the matrix effect. In fact, the emission of secondary ions is very sensitive to the chemical state of the sample surface [3,7,8]. Especially, depo-

sition and incorporation of electropositive elements drastically increases negative secondary ion yields on most surfaces. This increase of the analysis sensitivity can cover several orders of magnitude [9]. The deposition or incorporation of alkali metals (and in particular cesium) has been shown to decrease the electron work function of the sample [10–14] which induces an increase of the negative secondary ion sensitivity [15,16]. Hence, the negative secondary ion yields depend strongly on the stationary Cs surface concentration [9,15,17–19].

Because of the abovementioned reasons, Cs⁺ primary ion bombardment is widely used in SIMS analysis to effect this negative ion yield enhancement, thus providing higher detection sensitivities. On commercial dynamic SIMS instruments, this bombardment serves both for Cs incorporation into the sample and for sputtering. In such conditions, the primary ion bombardment conditions as well as the characteristics of the analyzed sample imply a distinct total sputtering yield, and consequently determine the Cs surface concentration. Hence, the Cs surface concentration is almost fixed for a given sample and an optimization of secondary ion yields is impossible. Studies examining

* Corresponding author. Tel.: +352 47 02 61 559; fax: +352 47 02 64.
E-mail address: philipp@lippmann.lu (P. Philipp).

the influence of the Cs surface concentration on negative secondary ion sensitivities were mainly limited to the evolution of the Cs surface concentrations in the transient regime or the surface concentrations obtained under different bombardment conditions [15,19].

The Cation Mass Spectrometer (CMS) is a SIMS prototype developed in our laboratory, which has been designed to overcome these problems [20–25]. The instrument is equipped with a neutral Cs^o evaporator [26] to vary the Cs surface concentration over the whole range and to ensure in that way an optimal Cs surface concentration for maximum MCs_x⁺ or negative secondary ion sensitivities. In such experimental conditions, the adjustment of the Cs surface concentration is decoupled from primary bombardment and the primary ion type can be chosen with respect to the application. Detailed studies on the evolution of negative secondary ion sensitivities [27] and the simulated Cs surface concentration with respect to the Cs deposition conditions [28] have been presented in previous papers.

In this paper, the energy distributions of the secondary ions studied in the previous papers [27,28] will be measured with respect to the experimental conditions. The sample will undergo ion bombardment with simultaneous neutral cesium Cs^o deposition. The relative variations of the electron work function will be extracted from that data and will be discussed with respect to the experimental conditions. By plotting the electron work function as a function of the simulated Cs surface concentration (the data of the previous paper is used, [28]), the experimental results obtained by ion irradiation and simultaneous Cs^o deposition can be compared to results in literature which were obtained for neutral Cs adsorption on various samples. Besides, a straight comparison of the experimental results with the electron-tunneling model, used to describe secondary ion emission from metallic and semi-conducting surfaces, is possible when plotting secondary ion yields with respect to the variations of the electron work function. Fundamental aspects linked to enhanced ion emission will be discussed and final conclusions regarding the influence of Cs^o deposition on ion emission can be drawn.

2. Experimental

The design and the main characteristics of the CMS have been published in previous works [20,21].

At the moment, the CMS is equipped with two ion guns and a patented neutral Cs^o evaporator which has been developed in our laboratory. The Ga⁺ LMIS was operated with an impact energy of 32.5 keV and primary beam currents between 100 pA and 5 nA. In order to vary the erosion rate and to adapt the Cs surface concentration, we changed the irradiation density with Ga⁺ ions by adjusting the dimensions of the scanned surface. The primary ion beam was thus raster-scanned across a quadratic area varying from 25 μm × 25 μm to 100 μm × 100 μm. The Cs⁺ sputter ion gun was run with an impact energy of 13 keV and primary beam currents ranging between 3 and 19 nA. The ion bombardment density was adjusted by varying the dimensions of the scanned area between 30 μm × 30 μm and 300 μm × 1200 μm. The neutral Cs deposition rates, which were measured by means

of a quartz microbalance system, were altered between 0.4 and 3.0 Å/s. During the experiments, the Cs^o deposition was used simultaneously with one of the aforementioned ion guns. The sample was positioned at a distance of 3.5 mm from the extraction lens.

The shifts of the work function are detected as a variation of the contact potential between the sample and the electrostatic analyser, which provokes a shift in the secondary ion energy spectra. In order to record these energy spectra, the sample potential, which is normally set to −4500 V for the analysis of negative secondary ions, was scanned from −4400 to −4520 V, while the remaining secondary optics remained unchanged. A good precision of the electron work function variations was obtained by reducing the energy bandwidth ΔE of the spectrometer from 130 to 2–3 eV. Experimentally, its accuracy has been determined to be equal to 0.15 eV [29]. The mass spectrometer was operated at a mass resolution of $M/\Delta M$ equal to 300.

For these series of measurements, secondary ions were accepted from a circular area on the sample surface limited to a diameter of 22 μm or 42 μm, defined by apertures of 400 μm or 750 μm diameter. The apertures were centred with respect to the scanned area. Cs is deposited on a larger area that is also centred on the irradiated area.

To study the electron work function variations with respect to the Cs surface concentration C_{Cs} and to observe the influence of the sample work function on ionization, we opted for samples of aluminium, silicon and nickel, given that these materials cover a considerable range of the work function scale: $\Phi_{Al} = 4.28$ eV [30], $\Phi_{Si} = 4.85$ eV [30] and $\Phi_{Ni} = 5.15$ eV [31]. These samples were compared to binary compounds (GaAs and InP). Only the work function of GaAs could be found in literature ($\Phi_{GaAs} = 5.3$ eV) [13]. Si, GaAs and InP were mono-crystalline samples, and thus ideal for a fundamental study of ionization processes, whereas Al and Ni were polycrystalline and thereby closer to industrial samples and to any future applications of the newly developed technique. For GaAs and Ni, important roughness formation has already been observed in the previous paper for Ga⁺/Cs^o bombardment, so that no experiments have been realized on those samples under given experimental conditions [27].

For a large number of erosion and Cs^o deposition rates, the energy distributions of the M[−] secondary ions were recorded on the five samples.

3. Results

3.1. Definitions

The energy distributions of secondary ions are recorded for different experimental conditions with defined erosion and Cs^o deposition rates. These conditions produce a Cs surface concentration that cannot be determined in situ. Therefore, this concentration will be described by characteristic parameters and it is considered to be a mean surface concentration in a volume close to the sample surface. These parameters have already been defined in a previous paper [27].

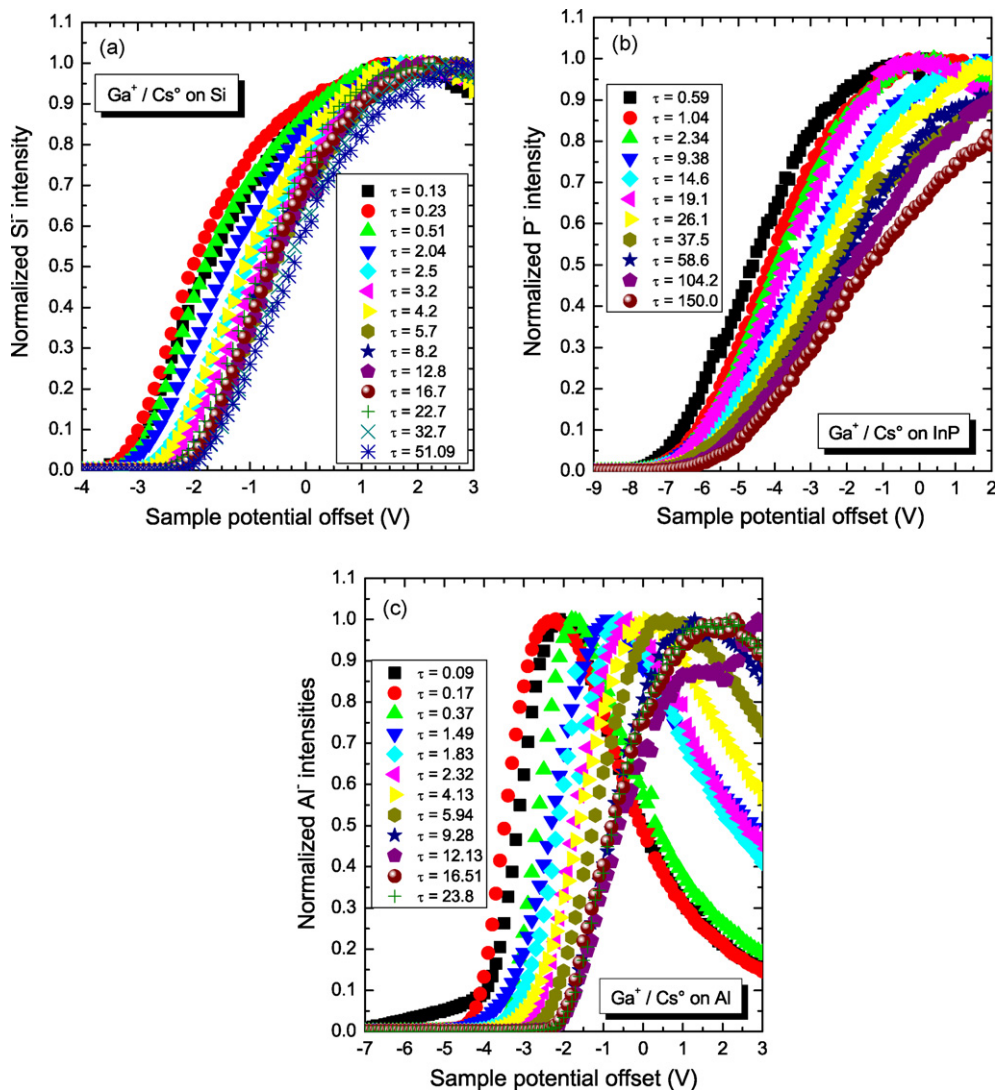


Fig. 1. Normalized energy distributions for $\text{Ga}^+/\text{Cs}^\circ$ bombardment with respect to the characteristic parameter τ : (a) on Si, (b) on InP, and (c) on Al.

For Ga^+ bombardment with simultaneous Cs° deposition ($\text{Ga}^+/\text{Cs}^\circ$ bombardment), the Cs surface concentration is characterized by the parameter τ which only depends on analytical parameters that can be determined easily [26,27]:

$$\tau = \frac{v_{\text{erosion}}}{v_{\text{deposition}}} \quad (1)$$

where v_{erosion} is the erosion velocity and $v_{\text{deposition}}$ is the Cs° deposition velocity. The erosion rate is calculated by taking the SIMS crater depth and the sputtering time into account and the Cs° deposition rate is measured by a quartz microbalance.

By analogy to relation (1), the Cs surface concentration for Cs^+ bombardment and simultaneous Cs° deposition ($\text{Cs}^+/\text{Cs}^\circ$ bombardment) is characterized by the parameter T [27]:

$$T = \frac{v_{\text{erosion}}}{v_{\text{deposition}}} \quad (2)$$

Due to additional Cs incorporation by the Cs^+ bombardment, a different parameter has to be defined for the $\text{Cs}^+/\text{Cs}^\circ$ bombardment than for the $\text{Ga}^+/\text{Cs}^\circ$ bombardment [27].

3.2. $\text{Ga}^+/\text{Cs}^\circ$ bombardment

Normalized energy distributions of negative secondary ions sputtered from Si, InP and Al surfaces under $\text{Ga}^+/\text{Cs}^\circ$ bombardment are shown in Fig. 1 (zoom on the low-energy region of the spectra). They have been recorded for the parameter τ varied over a large range. For the InP sample, P^- ions have been detected because they present a much higher secondary ion ionization probability than In. Fig. 1 shows that for varying values of τ , the whole energy distributions are shifted with respect to the energy axis while their shape mainly remains unchanged.

The relative variations of the electron work function can be extracted from the energy distributions by fitting the low-energy part of the distributions with tangents (part of fast increase which is represented in Fig. 1). The intercepts of the tangents with the energy axis were chosen as a marker of the spectra position and used for the evaluation of the work function variations [32,33,15,34]. The curve obtained for the highest value of τ , for example τ equal to 51.1 for Si (Fig. 1a), corresponds to the experimental conditions of lowest Cs surface concentration and

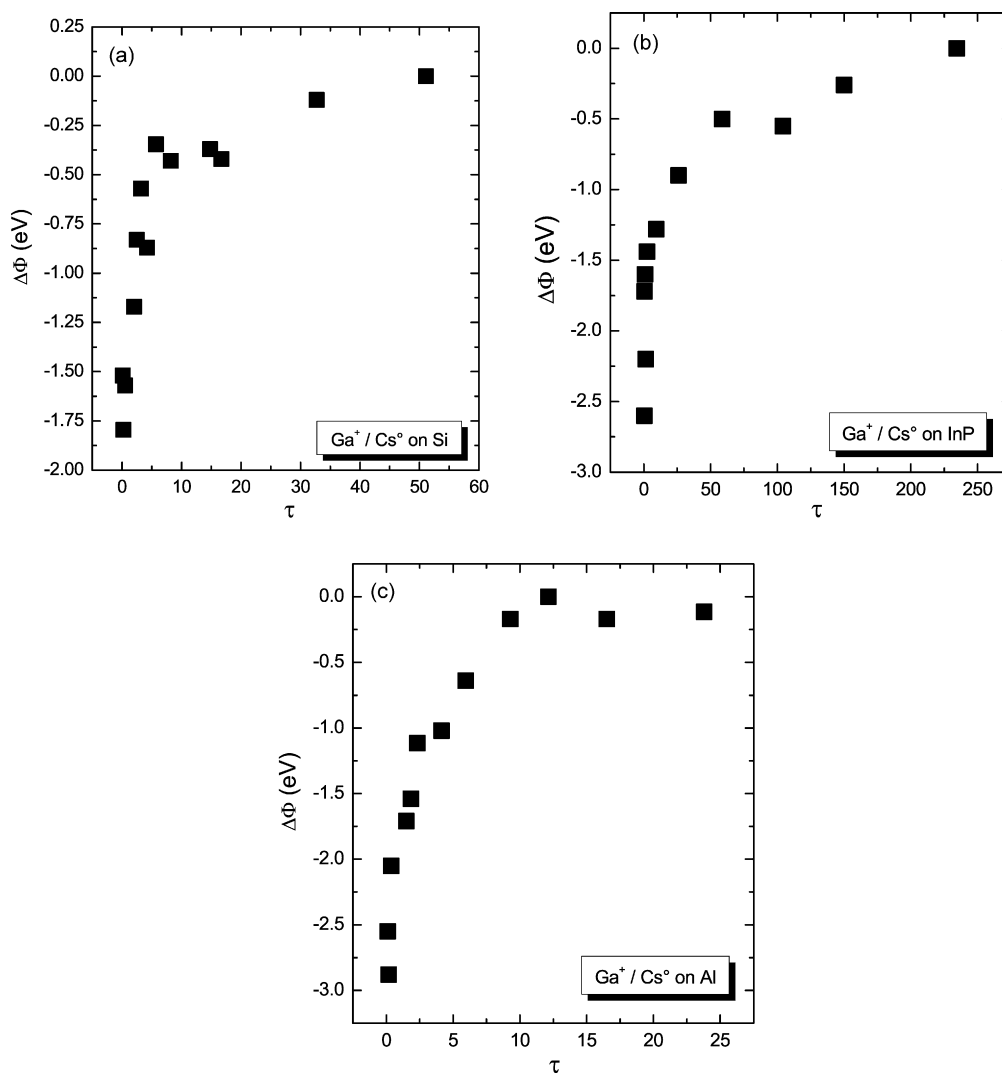


Fig. 2. Relative variations of electron work function Φ with respect to the parameter τ for $\text{Ga}^+/\text{Cs}^\circ$ bombardment: (a) on Si, (b) on InP, and (c) on Al.

is defined as origin of the relative work function variations. The shifts of the other curves with respect to that curve define the relative variations of the electron work function induced by the Cs° deposition. The electron work function shifts with respect to the characteristic parameter τ have been plotted in Fig. 2 for the Si, InP and Al samples.

The different work function curves of Fig. 2 show a similar behavior. For high values of τ , and thus for small Cs surface concentrations, the electron work function Φ is almost not reduced. This reduction becomes more important for small values of τ (high Cs surface concentrations). The maximum decrease of Φ depends on the sample. For Si, the maximum decrease is of -1.8 eV while it is of -1.7 eV for InP and of -2.8 eV for Al.

Next, the electron work function is plotted with respect to the Cs surface concentrations which have been calculated by the simulation code TRIDYN in a previous paper (Fig. 3) [28]. The simulated concentrations obtained by TRIDYN gave only approximate values of the Cs surface concentration C_{Cs} . Nevertheless they allow to compare the variations of the electron work function as a function of the Cs surface concentration to

experimental results found in literature for the adsorption of Cs on different samples (without ion irradiation, and thus no perturbation of the sample surface) [10,11,13,35].

As shown in Fig. 3, at 0 concentration (work function of the virgin sample) the values of the electron work function Φ have been obtained by linear extrapolation from the small concentrations [36]. So the values indicated are no longer relative changes of Φ , but absolute variations of that parameter. At small concentrations, the electron work function Φ of Si decreases steeply to a value of -1.2 eV (Fig. 3a). This decrease cannot be observed on curves for Cs adsorption in general [11,13,35] and is probably due to errors in the calculations of the parameter τ [28] as well as to the limits of the simulation of the Cs surface concentration [28]. For higher C_{Cs} , the decrease is more moderate and the maximum decrease of Φ at -1.8 eV is reached at C_{Cs} equal to 0.41. Afterwards Φ increases slightly to reach a final value of -1.5 eV at C_{Cs} equal to 0.58. This behaviour is characteristic for metals and is also found for Si [35,37].

In the case of InP (Fig. 3b), a steep decrease of Φ at C_{Cs} close to 0 is also observed. The explanations for this behaviour are the

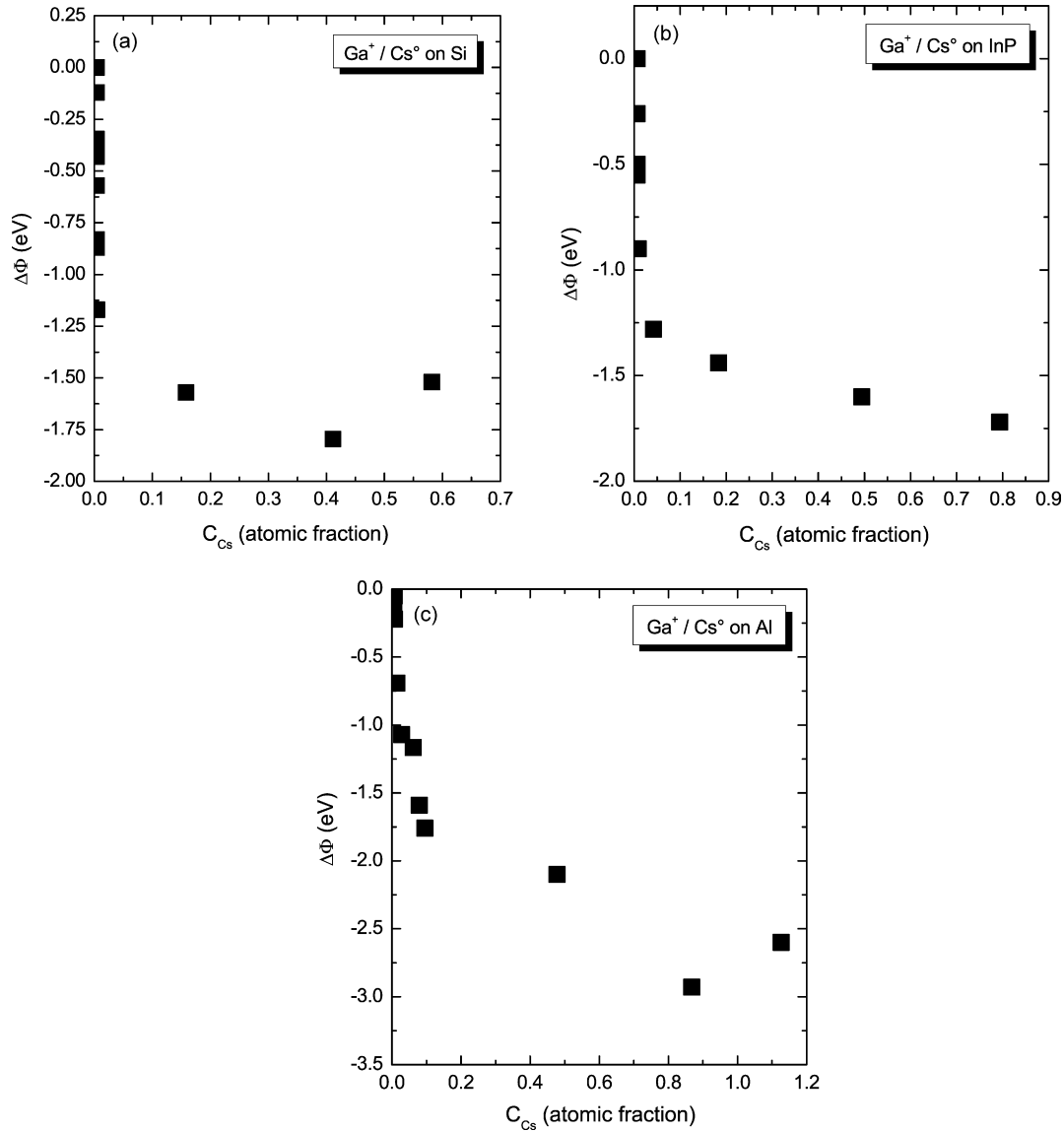


Fig. 3. Variations of electron work function Φ with respect to the Cs surface concentration for Ga^+/Cs^+ bombardment: (a) on Si, (b) on InP, and (c) on Al.

same than for Si. Towards higher C_{Cs} , Φ decreases constantly and no minimal value is reached. This is observed for Cs adsorption on semi-conductors in general [13,38]. Experimentally, the largest decrease of Φ ($\Delta\Phi = -1.7$ eV) is observed at C_{Cs} equal to 0.8.

The Al sample behaves similarly than Si (Fig. 3c). The minimal Φ ($\Delta\Phi = -2.9$ eV) is reached at C_{Cs} equal to 0.87. Afterwards Φ increases slightly up to a relative value of -2.6 eV. This slight increase is expected for metals [11], but it can also be produced by instabilities in the electronics of the CMS instrument. C_{Cs} larger than 1 are due to the extrapolation at low values of τ and have been discussed in a previous paper [28].

In a previous paper, the sensitivities of negative secondary ions have been discussed in terms of useful yield which has been defined by [27]:

$$\text{UY}(\text{M}^-) = \frac{\text{number of detected } \text{M}^- \text{ ions}}{\text{number of sputtered M atoms}} \quad (3)$$

In that paper, the useful yield has been discussed with respect to the parameter τ . However, plotting the useful yield with respect to the variations of Φ is substantial in order to compare the experimental results to the electron-tunneling model describing ion emission from metallic and semi-conducting surfaces. The electron-tunneling model is given by the following equation:

$$\begin{cases} \beta_{\text{M}}^- = 1, & \text{if } \phi < A \\ \beta_{\text{M}}^- \propto e^{-((\phi-A)/\varepsilon_n)}, & \text{if } \phi > A \end{cases} \quad (4)$$

where β_{M}^- is the secondary ion ionization probability, Φ the electron work function of the sample, A the electron affinity of the sputtered atom and ε_n is proportional to the normal component of the velocity with which the sputtered atom leaves the sample surface. The deposited Cs decreases Φ . The useful yield, which is proportional to β_{M}^- , varies exponentially with Φ .

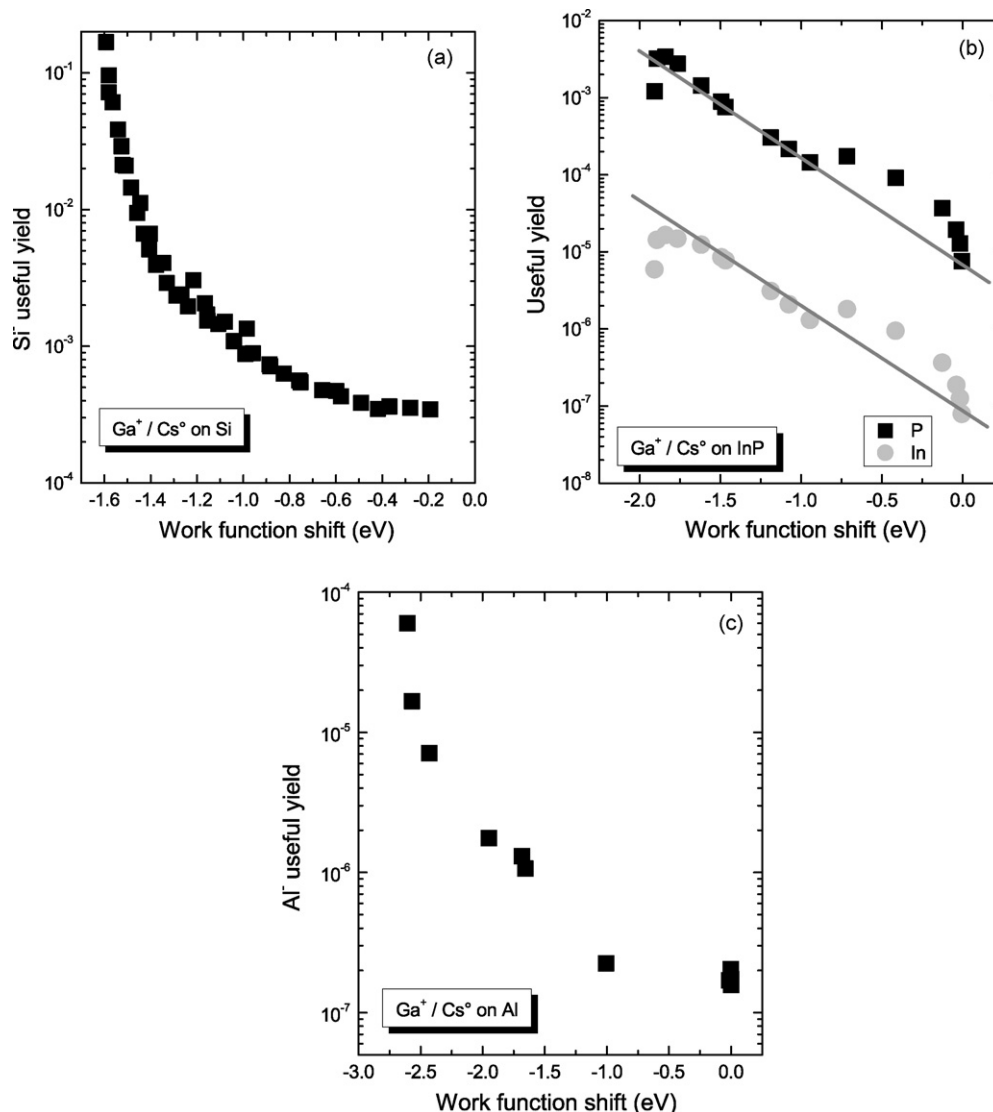


Fig. 4. Useful yield variation with respect to the electron work function for Ga⁺/Cs[°] bombardment: (a) on Si, (b) on InP, and (c) on Al.

This behavior is plotted in Fig. 4 for the Si, InP and Al samples. The useful yield values have been taken from a previous paper [27]. Here they have been represented as a function of the variations of Φ which have been obtained in this work. For Si (Fig. 4a), the useful yield is smallest for the work function value of the virgin sample and increases by almost three orders of magnitude for decreasing values of Φ . The electron-tunneling model predicts an exponential increase of the useful yield for a decreasing Φ , which cannot be observed for Si. On Fig. 4b, the useful yields of In⁻ and P⁻ increase exponentially for decreasing values of Φ . This behaviour corresponds to the electron-tunneling model for Φ larger than the electron affinity of In and P. However a saturation of the useful yields, corresponding to the predictions of the electron-tunneling model when Φ becomes smaller than the electron affinity, cannot be observed. Probably the Φ decrease induced by the deposition of Cs is not important enough. Nevertheless, a sensitivity increase of three orders of magnitude is obtained.

On the Al sample (Fig. 4c), a similar behaviour than for Si is observed.

3.3. Cs⁺/Cs[°] bombardment

The normalized energy distributions for Cs⁺/Cs[°] bombardment on Si, GaAs, InP, Al and Ni are shown in Fig. 5 (zoom on the low-energy region of the spectra). Like for Ga⁺/Cs[°] bombardment, they have been recorded for the characteristic parameter T varied over a large range. Negative secondary ions giving rise to the highest intensities have been chosen: for GaAs As⁻ ions have been detected and for InP P⁻ ions have been selected. At small energies (high negative sample potentials), secondary ion intensities increase rapidly. A similar behaviour is found on all samples. The slow decrease of the energy distributions at higher energies is not shown because it is of no interest for the evaluation of the electron work function evolutions. The same method than for Ga⁺/Cs[°] bombardment has been used to extract

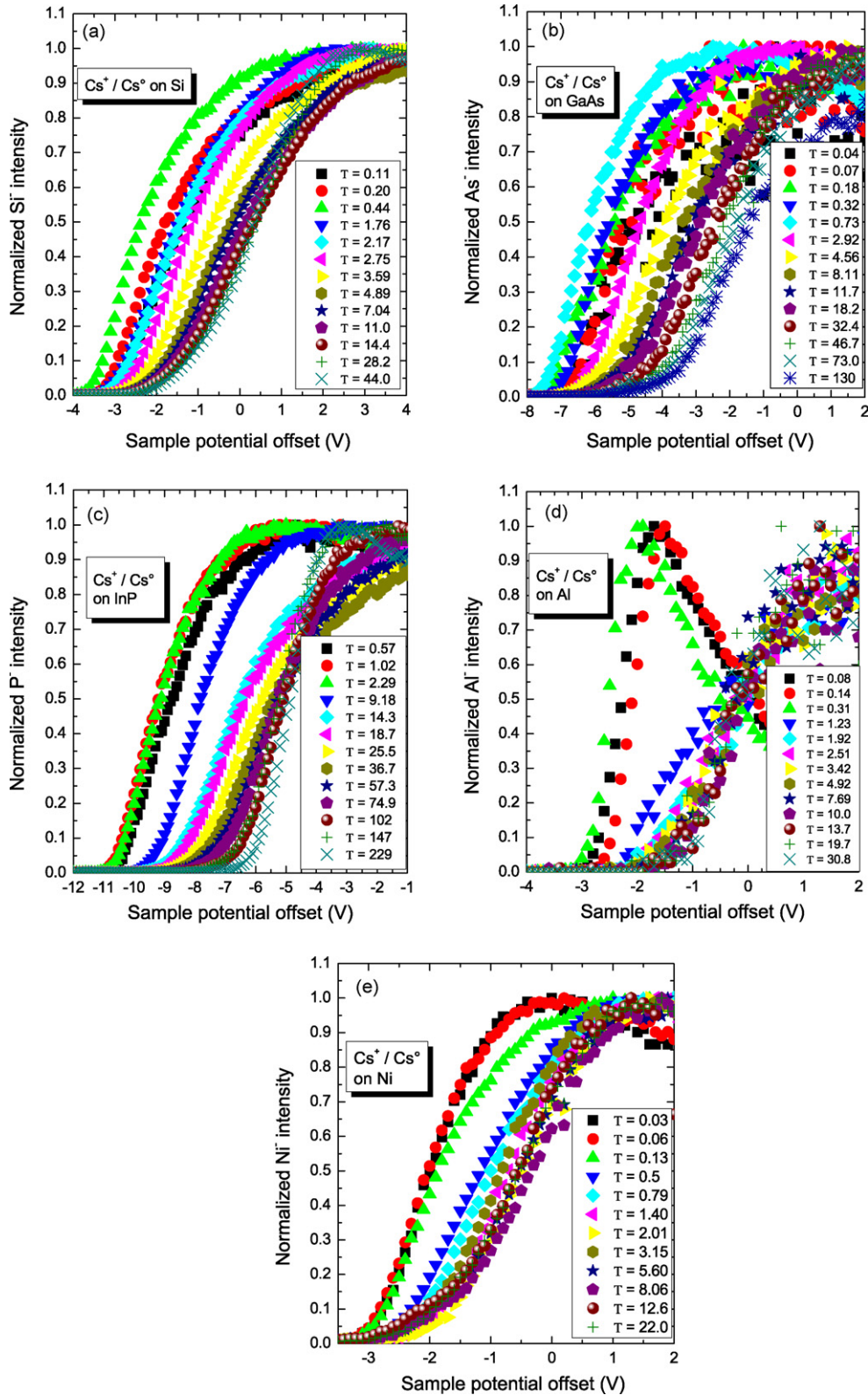


Fig. 5. Normalized energy distributions for $\text{Cs}^+/\text{Cs}^\circ$ bombardment with respect to the characteristic parameter T (a) on Si, (b) on GaAs, (c) on InP, (d) on Al, and (e) on Ni.

these variations of the electron work function Φ from the energy distributions.

The variations of Φ are shown in Fig. 6. At high values of the characteristic parameter T , Φ is almost constant, while it

decreases rapidly at high C_{Cs} (small values of T). The maximum decrease of Φ depends on the sample, as observed for $\text{Ga}^+/\text{Cs}^\circ$ bombardment. This maximum decrease of Φ is equal to -2.8 eV for Si (Fig. 6a), while higher decreases are observed for GaAs

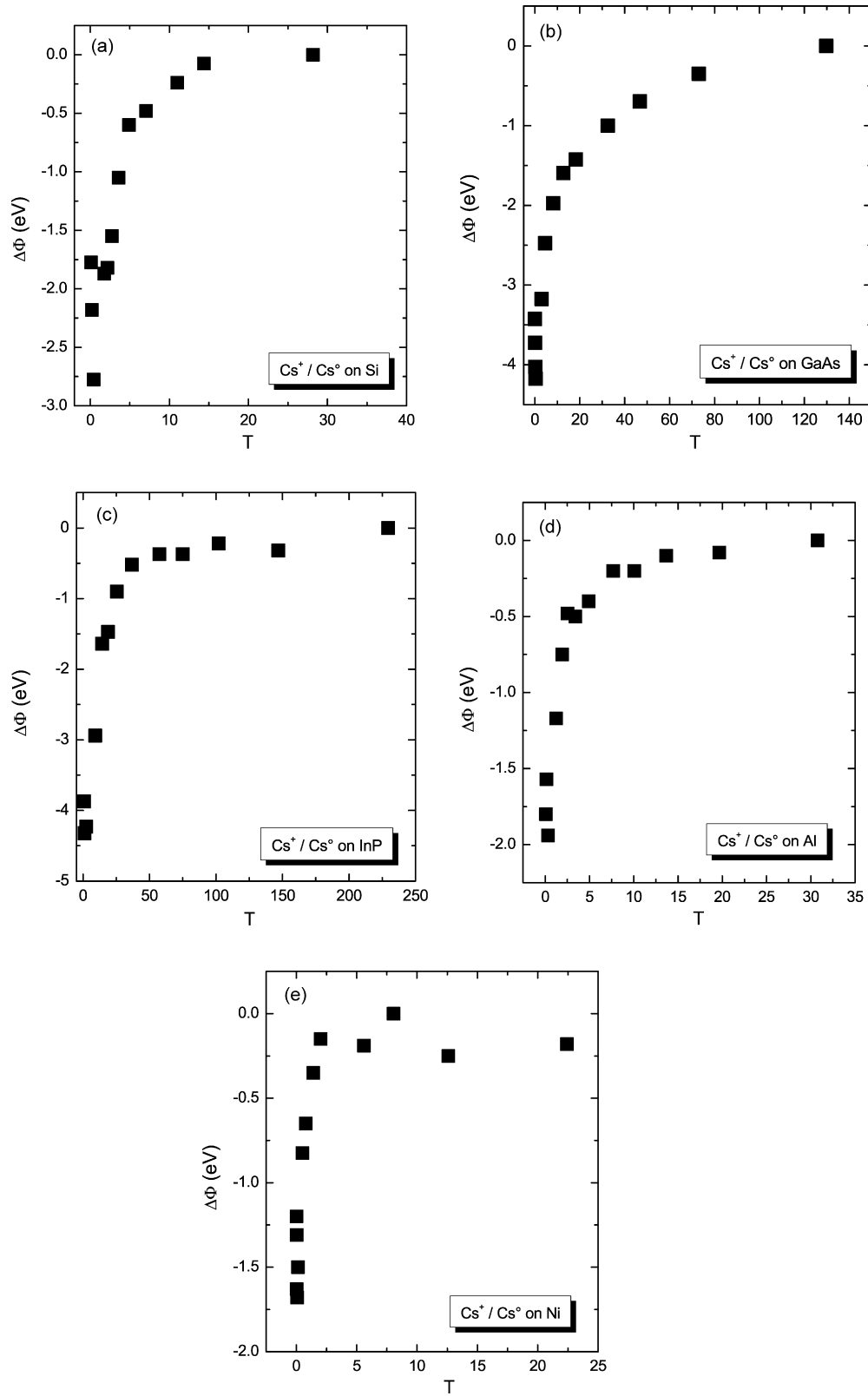


Fig. 6. Relative variations of electron work function Φ with respect to the parameter T for $\text{Cs}^+/\text{Cs}^\circ$ bombardment: (a) on Si, (b) on GaAs, (c) on InP, (d) on Al, and (e) on Ni.

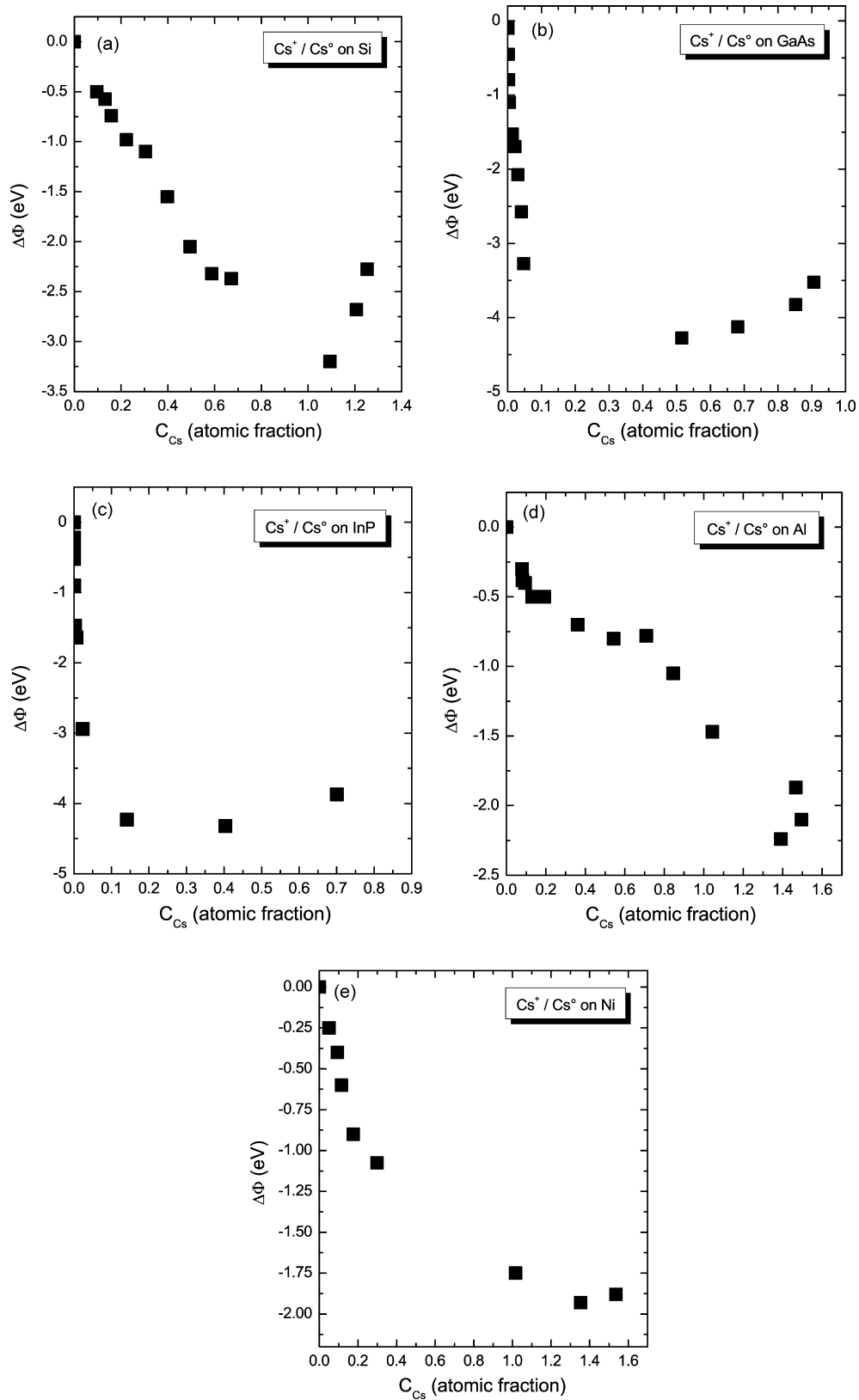


Fig. 7. Variations of electron work function Φ with respect to the Cs surface concentration for Cs⁺/Cs[°] bombardment: (a) on Si, (b) on GaAs, (c) on InP, (d) on Al, and (e) on Ni.

($\Delta\Phi = -4.7$ eV, Fig. 6b) and InP ($\Delta\Phi = -4.3$ eV, Fig. 6c). For Al and Ni, maximum decreases of -1.9 and -2.4 eV are observed (Fig. 6d and e).

Next, Φ is plotted with respect to C_{Cs} which has been simulated by the TRIDYN code in a previous paper [28] (Fig. 7). Values of Φ for C_{Cs} equal to 0 have been obtained by extrapolation from the small Cs surface concentrations [32,33,15,34]. As already mentioned, TRIDYN gave only approximate values of C_{Cs} , which nevertheless allow to compare the variations of Φ as a function of C_{Cs} to experimental results found in the literature.

For Si (Fig. 7a), Φ decreases constantly until reaching the minimal value of -3.2 eV at C_{Cs} equal to 1.1. Afterwards it increases slightly up to a decrease of -2.3 eV. This behaviour of Si has also been found in literature for Cs adsorption on Si [35,37]. C_{Cs} larger than 1 is due to an extrapolation at small values of T , which has already been discussed in a previous paper [28].

As shown in Fig. 7b Φ of the GaAs sample decreases extremely rapidly down to a relative value of -3.3 eV. This steep decrease has not been observed in literature for Cs adsorption on semi-conductors [35,37,38], and GaAs in particular [13]. It is probably due to uncertainties in C_{Cs} obtained by simulations using the TRIDYN code [28]. The small increase of Φ at C_{Cs} higher than 0.9 is probably due to shifts in the CMS electronics. For the InP sample, a similar behaviour than for the GaAs sample has been found (Fig. 7c).

For Al (Fig. 7d), Φ decreases constantly with increasing C_{Cs} without reaching a minimum. Apparently the Cs deposition does not allow to reach the lowest Φ that are possible on Al.

On the Ni sample (Fig. 7e), Φ decreases rather steeply for values of C_{Cs} varying between 0 and 0.35. For higher Cs surface concentrations, the Φ decrease becomes more moderate and reaches the minimal value of -1.9 eV at C_{Cs} equal to 1.35. A small increase of Φ for higher C_{Cs} cannot be identified clearly. This is expected for metals and for Ni in particular at high C_{Cs} [31].

Identically to Ga^+/Cs° bombardment, the useful yields of secondary ions sputtered from the different samples are plotted with respect to the electron work function in order to compare the experimental results to the electron-tunneling model. Details have been given in the previous paragraph. The results for Cs^+/Cs° bombardment are shown in Fig. 8.

As shown in Fig. 8a, this behaviour of Si^- corresponds to the predictions of the electron-tunneling model for Φ larger than the electron affinity of the sputtered atom. A saturation of the useful yields, indicating total ionization of the sputtered atoms (when Φ smaller than the electron affinity of the sputtered atom) cannot be observed. The decrease of Φ induced by the deposition of Cs results in a useful yield increase of about two orders of magnitude.

The useful yield variations of Ga^- and As^- are plotted in Fig. 8b. No saturation of the useful yields can be observed. This has been expected because As and Ga have lower electron affinities than Si. A similar behaviour has been found for the InP sample (Fig. 8c). Therefore the explanations for the GaAs sample are also valid for this sample.

The Al sample (Fig. 8d) shows a similar behaviour than Si however the useful yield gain induced by the decrease of Φ is limited to 1.5 orders of magnitude.

On the Ni sample (Fig. 8e), the Ni^- useful yield decreases only moderately for the smallest values of Φ (variations of Φ ranging from -1.6 to -0.8 eV). This decrease becomes only exponential for variations of Φ smaller than -0.8 eV. The second part of the curve with the exponential variations of the useful yield corresponds to the predictions of the electron-tunneling model when Φ is larger than the electron affinity of Ni, while the almost constant useful yield values correspond to the predictions when Φ is smaller than the electron affinity. The smooth crossover from one part of the model to the other is explained by the influence of parameters other than Φ and the electron affinity [39,40].

4. Discussion

4.1. Comparison of Φ variations for Ga^+/Cs° and Cs^+/Cs° bombardment

The variation of the electron work function with respect to the characteristic parameters τ and T is similar for both types of ion bombardments. A small decrease of Φ is observed for high values of τ and T and gets more important towards smaller values of τ and T (and thus for higher Cs surface concentrations) to present a steep decrease at highest Cs surface concentrations. For Ga^+/Cs° and Cs^+/Cs° bombardment on the same sample, different values for the maximum decrease of Φ have been obtained (Table 1). For a number of samples, these differences are important. This can be seen for example in the case of InP ($\Delta\Phi = -1.7$ eV for Ga^+/Cs° bombardment compared to $\Delta\Phi = -4.3$ eV for Cs^+/Cs° bombardment). These fluctuations are due to different maximum Cs surface concentrations. On the one hand, C_{Cs} rapidly increases for small values of τ and T [27] and a small fluctuation of C_{Cs} can induce an important variation of Φ (Figs. 3 and 7). On the other hand, the experimental series had to be realized in a short time period in order to avoid any shifts in the electronics which could produce a shift on the mass spectrometer voltages. This voltage shift would add to the work function shift and falsify the experimental results. Especially for the small values of τ and T , the acquisition times could be too short in order to guarantee the experiments to be realized beyond the pre-equilibrium regime. In fact, for small values of τ and T , the Cs deposition rates get important compared to the erosion rates which lengthens the transient regime.

Table 1

Relative decrease of the electron work function for the Si, GaAs, InP, Al and Ni samples obtained for Ga^+/Cs° and Cs^+/Cs° bombardments

	Ga^+/Cs° bombardment (eV)	Cs^+/Cs° bombardment
Si	-1.8	-2.8
GaAs	-	-4.1
InP	-1.7	-4.3
Al	-2.8	-1.9
Ni	-	-1.7

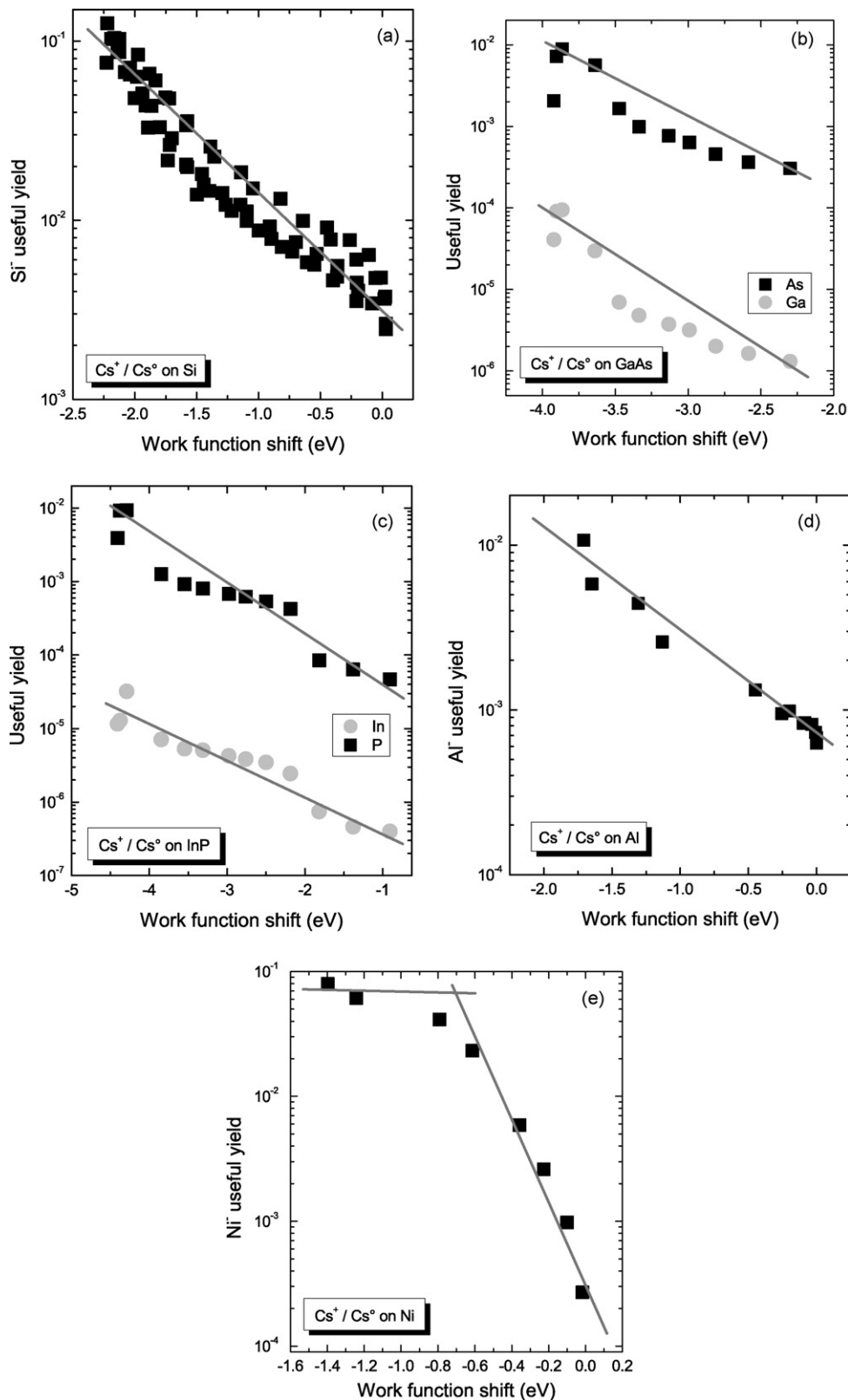


Fig. 8. Useful yield variation with respect to the electron work function for $\text{Cs}^+/\text{Cs}^\circ$ bombardment: (a) on Si, (b) on GaAs, (c) on InP, (d) on Al, and (e) on Ni.

4.2. Comparison of Φ variations with results from literature

The variations of the electron work function with respect to the Cs surface concentration, which have been obtained for

$\text{Ga}^+/\text{Cs}^\circ$ and $\text{Cs}^+/\text{Cs}^\circ$ bombardment, will be compared to each other and to values found in literature. For most samples, no significant differences between the $\text{Ga}^+/\text{Cs}^\circ$ and the $\text{Cs}^+/\text{Cs}^\circ$ bombardment can be seen for the work function variations with

Table 2

Maximal electron work function decrease in eV for Si, GaAs, InP, Al and Ni samples [11,12,30,36,40,41] under Ga⁺/Cs[◦] and Cs⁺/Cs[◦] bombardment conditions and for values found in literature

	Ga ⁺ /Cs [◦] bombardment (eV)	Cs ⁺ /Cs [◦] bombardment (eV)	Literature
Si	−1.8	−3.2	−3.4 to −3.6 eV [36,40]
GaAs	−	−4.2	−2.6 to −3.6 eV [12,41]
InP	−1.7	−4.3	−
Al	−2.9	−2.2	−2.4 eV [11]
Ni	−	−1.9	−3.1 eV [30]

respect to the Cs surface concentration. A fast decrease of Φ at low C_{Cs} is followed by minimal values of Φ and for some samples with a small increase of Φ at the highest C_{Cs} .

During our experiments, the most important decrease of Φ on Si has been obtained for Cs⁺/Cs[◦] bombardment (maximal decrease of −3.2 eV compared to −1.8 eV for Ga⁺/Cs[◦] bombardment). The value of $\Delta\Phi$ equal to −3.2 eV is comparable to the maximal values of $\Delta\Phi$ that have been obtained in literature (−3.2 to −3.6 eV, Table 2) [37,41]. So C_{Cs} has almost been optimized during our study in order to minimize Φ and obtain maximal Si[−] useful yields.

For the GaAs sample, only the results from Cs⁺/Cs[◦] bombardment can be compared to the values from literature. The maximal decrease of −4.2 eV obtained experimentally is below the maximal values that have been found in literature and which cover the range from −2.6 eV (GaAs(001), [12]) to −3.6 eV (GaAs(110), [42]) (Table 2). Possibly, the difference is due to target modification by ion bombardment with simultaneous Cs[◦] deposition and thereby induced roughness formation in the irradiated area.

Experimentally, the Φ decrease obtained on InP by Cs⁺/Cs[◦] bombardment (−4.3 eV) is significantly larger than the maximal decrease obtained by Ga⁺/Cs[◦] bombardment (−1.7 eV). No values for a maximal decrease of Φ have been found in the literature so that the accuracy of the experimental values cannot be verified (Table 2).

On the Al sample, the Ga⁺/Cs[◦] bombardment produces a decrease of Φ down to a minimal value followed by a small increase, while the Cs⁺/Cs[◦] bombardment implies a constant decrease of Φ (Fig. 3c and 7d). Besides, the largest decrease of Φ has been obtained for Ga⁺/Cs[◦] bombardment (−2.9 eV compared to −2.2 eV for Cs⁺/Cs[◦] bombardment). This is slightly larger than the maximal decrease of −2.4 eV which has been found for Cs[◦] deposition on Al(111) (Table 2) [11]. However, the differences between experimental values obtained by ion bombardment with simultaneous Cs[◦] deposition and the value from literature is rather small. The slightly higher Φ decrease obtained for Ga⁺/Cs[◦] bombardment is probably due to the surface roughness that has been induced by the Ga⁺ bombardment and which is significantly larger than the roughness obtained by Cs⁺ bombardment [27].

On the Ni sample, the decrease for the Cs⁺/Cs[◦] bombardment is limited to −1.9 eV. The observed maximal decrease is largely smaller than the value found in literature (−3.1 eV) [31] (Table 2). The difference between the value that has been obtained experimentally and the value taken out of literature is either due the polycrystalline Ni sample we used or to the too

low Cs surface concentration. In fact, the electron work function depends on the crystalline orientation and on a polycrystalline sample this orientation is averaged over several grains.

4.3. Useful yield variations as a function of Φ

The useful yield variations with respect to the electron work function have been plotted in Figs. 4 and 8. For Si, both bombardment types produce different behaviours. For the Cs⁺/Cs[◦] bombardment, the Si[−] useful yield decreases exponentially with respect to the increasing electron work function which agrees with the predictions of the electron-tunneling model, while the decrease of the Si[−] useful yield for Ga⁺/Cs[◦] bombardment is not linear on the semi-log scale. The useful yield of Si[−] decreases steeply for the lowest values of Φ and changes to almost constant values at high values of Φ . Besides, for both types of primary ions constant useful yield values indicating Φ smaller than the electron affinity cannot be seen. For both bombardments, the decrease of Φ induced by the deposition of C_{Cs} is not important enough. Nevertheless, as already discussed in a previous paper [27], the ionization of sputtered Si must be total or at least almost total, showing that the deposition of Cs decreased the value of Φ closely to the electron affinity of Si.

The Al sample shows an exponential decrease of the useful yield for the Cs⁺/Cs[◦] bombardment (linear decrease on semi-log scale) and a steep decrease at low values of Φ and almost constant useful yields at high values of Φ for the Ga⁺/Cs[◦] bombardment. As Al and Si show a similar behaviour, an influence of the primary ion type on the decrease of Φ with respect to C_{Cs} cannot be excluded. They could derive from a different mixing of the deposited Cs atoms with the atoms of the sample for both types of primary ions.

In contrast to the results obtained for Si[−] and Al[−] ions, no significant differences have been observed on the InP sample for both types of primary bombardment. As well for the Ga⁺/Cs[◦] bombardment as for the Cs⁺/Cs[◦] bombardment, the useful yields of In[−] and P[−] decrease exponentially with increasing values of Φ . Fluctuations on the curves are probably due to uncertainties in the useful yield evaluation and the work function measurement. So, besides the primary ion type, the sample composition has probably also an influence on the variation of Φ with respect to Cs deposition.

For the Ni and GaAs samples, only results for the Cs⁺/Cs[◦] bombardment have been obtained. The useful yields of As[−] and Ga[−] show a similar behaviour than the useful yields of P[−] and In[−]. The useful yield of Ni[−] shows a distinct behaviour from the other samples with almost constant useful yield values at low

values of Φ and an exponential decrease at higher values of Φ . It matches the predictions of the electron-tunneling model.

Our results of the work function evaluation indicate that the $\text{Cs}^+/\text{Cs}^\circ$ bombardment produces exponential variations of the useful yields for all elements. Only for Ni, the results agree with the predictions of the electron-tunneling model (constant useful yields at low work function values and exponential decrease at higher values of Φ). For Al, the roughness formation at the crater bottom influences results. The semi-conductor Si, with a higher electron affinity and a lower electron work function than Ni, shows no constant useful yield values at low values of Φ , while smaller values of Φ than for Ni have been reached. For the Si and Al sample, the differences with the electron-tunneling model are even larger for the $\text{Ga}^+/\text{Cs}^\circ$ bombardment than for the $\text{Cs}^+/\text{Cs}^\circ$ bombardment. Almost no differences between both ion bombardments can be seen for the InP sample. Besides the primary ion type and the atomic mixing of Cs, the roughness formation at the crater bottom for certain experimental conditions, especially for polycrystalline samples, must be taken into account.

5. Conclusion

For several samples, the energy distributions of secondary ions have been recorded under Ga^+ bombardment with simultaneous Cs° deposition and under Cs^+ bombardment with simultaneous Cs° deposition in order to calculate the decrease of the electron work function induced by the deposition of Cs and to quantify the influence of Cs deposition on the useful yield increases. The electron work functions have been plotted with respect to several parameters. In that way, they could be discussed with respect to the experimental conditions and compared to work function variations taken from literature and which have been obtained for Cs adsorption (without ion irradiation) on several samples. A comparison with the electron-tunneling model becomes possible after plotting the useful yields with respect to the work function variations.

In that way, the increase of the useful yields, which have already been observed for the deposition of Cs in a previous paper, could be explained by the decrease of the electron work function. It has been shown that the deposition of Cs induces a decrease of the sample work function which then produces a gain of the useful yield. In general, this behaviour can be predicted by the electron-tunneling model and by the data available for the adsorption of Cs on different samples. In contrast to the experimental conditions of Cs adsorption, the Cs atoms were partially introduced into the sample by atomic mixing under Ga^+ and Cs^+ bombardment in this work.

Similar behaviours between our experimental work function variations and Cs adsorption curves taken from literature have been found. However, minimal values of the work function as well as the shape of the curves did not match for all samples or bombardment conditions. Differences are partially due to dissimilarities in atomic mixing and thereby induced roughness formation on the crater bottom under ion irradiation and to uncertainties in the evaluation of the Cs surface concentration or the characteristic parameters τ and T . The useful yield

variations with respect to the work function variations matched also partially the predictions of the model, especially for Ni. For other samples, only the exponential decrease of the useful yield was observed. No constant useful yields for low values of the work function have been observed, and for some samples the decrease was not linear on a semi-log scale. These differences are due to the factors mentioned above. The primary ion type as well as the sample composition influence the atomic mixing of Cs and influence probably the variation of the electron work function. The evaluation of the experimental data is also complicated by the formation of roughness formation on the crater bottoms.

Nevertheless, ion bombardment with simultaneous Cs deposition increases much the sensitivity of SIMS by several orders of magnitude, which can be attributed to a work function decrease induced by the deposition (and the incorporation into the sample) of cesium. The behaviour at maximal Cs surface concentrations and for different types of primary ions and sample compositions has to be verified.

Acknowledgment

This work has been supported by the “Ministère de la Culture, de l’Enseignement Supérieur et de la Recherche” of Luxembourg.

References

- [1] M.G. Dowsett, R.D. Barlow, *Anal. Chim. Acta* 297 (1994) 253.
- [2] P.C. Zalm, *Rep. Prog. Phys.* 58 (1995) 1321.
- [3] G. Stinger, *Anal. Chim. Acta* 297 (1994) 231.
- [4] J.-N. Audinot, S. Schneider, M. Yegles, P. Hallegot, R. Wennig, H.-N. Migeon, *Appl. Surf. Sci.* 231/232 (2004) 490.
- [5] R. Levi-Setti, K.L. Gavrilov, P.L. Strissel, R. Strick, *Appl. Surf. Sci.* 231/232 (2004) 479.
- [6] S. Chandra, *Appl. Surf. Sci.* 231/232 (2004) 462.
- [7] H.A. Storms, K.F. Brown, J.D. Stein, *Anal. Chem.* 49 (1977) 2023.
- [8] M.A. Karolewski, R.G. Cavell, *Appl. Surf. Sci.* 193 (2002) 11.
- [9] K. Wittmaack, *Surf. Sci.* 126 (1983) 573.
- [10] M. Scheffler, C. Stampfl, Theory of adsorption on metal substrates. In: *Handbook of Surface Science*, vol. 2: Electronic Structure, (Eds.) K. Horn, M. Scheffler. Elsevier, Amsterdam 2000. 286–356.
- [11] A. Hohlfeld, M. Sunjic, K. Horn, *J. Vac. Sci. Technol. A* 5 (4) (1987) 679.
- [12] B. Kierren, D. Paget, *J. Vac. Sci. Technol. A* 15 (4) (1997) 2074.
- [13] D. Heskett, T. Maeda, A.J. Smith, W.R. Graham, N.J. DiNardo, E.W. Plummer, *J. Vac. Sci. Technol. B* 7 (4) (1989) 915.
- [14] P. Soukiassian, L. Spiess, K.M. Schirm, P.S. Mangat, J.A. Kubby, S.P. Tang, A.J. Freeman, *J. Vac. Sci. Technol. B* 11 (4) (1993) 1431.
- [15] H. Gnaser, *Phys. Rev. B* 54 (23) (1996) 16456.
- [16] T. Kan, K. Mitsukawa, T. Ueyama, M. Takada, T. Yasue, T. Koshikawa, *J. Surf. Anal.* 5 (1) (1999) 52.
- [17] P.A.W. van der Heide, *Appl. Surf. Sci.* 157 (2000) 191.
- [18] H. Gnaser, *Phys. Rev. B* 63 (2001) 45425.
- [19] P.A.W. van der Heide, *Nucl. Instrum. Meth. Phys. Res. B* 194 (2002) 489.
- [20] T. Mootz, B. Rasser, P. Sudraud, E. Niehuis, T. Wirtz, W. Bieck, H.-N. Migeon, in: A. Benninghoven, P. Bertrand, H.-N. Migeon, H.W. Werner (Eds.), *Secondary Ion Mass Spectrometry SIMS XII*, Elsevier, Amsterdam, 2000, p. 233.
- [21] T. Wirtz, B. Duez, H.-N. Migeon, H. Scherrer, *Int. J. Mass Spectrom.* 209 (2001) 57.
- [22] P. Philipp, T. Wirtz, H.-N. Migeon, H. Scherrer, *Appl. Surf. Sci.* 231/232 (2004) 754.

- [23] T. Wirtz, H.-N. Migeon, H. Scherrer, *Int. J. Mass Spectrom.* 225 (2003) 135.
- [24] T. Wirtz, H.-N. Migeon, *Surf. Sci.* 557 (2004) 57.
- [25] T. Wirtz, H.-N. Migeon, *Surf. Sci.* 561 (2004) 200.
- [26] T. Wirtz, H.-N. Migeon, *Appl. Surf. Sci.* 231/232 (2004) 940.
- [27] P. Philipp, T. Wirtz, H.-N. Migeon, H. Scherrer, *Int. J. Mass Spectrom.* 253 (2006) 71.
- [28] P. Philipp, T. Wirtz, H.-N. Migeon, H. Scherrer, *Int. J. Mass Spectrom.* 261 (2007) 91.
- [29] T. Wirtz, PhD thesis, INPL, 2002.
- [30] H.B. Michaelson, *J. Appl. Phys.* 48 (11) (1977) 4729.
- [31] R.L. Gerlach, T.N. Rhodin, *Surf. Sci.* 19 (1970) 403.
- [32] M. Bernheim, F. Le Bourse, *Nucl. Instrum. Meth. Phys. Res. B* 27 (1987) 94.
- [33] M. Bernheim, G. Slodzian, in: A. Benninghoven, A.M. Huber, H.W. Werner (Eds.), *Secondary Ion Mass Spectrometry SIMS VI*, Wiley & Sons, Chichester, 1988, p. 139.
- [34] H. Gnaser, *Phys. Rev. B* 54 (23) (1996) 17141.
- [35] J.E. Ortega, E.M. Oellig, J. Ferrón, R. Miranda, *Phys. Rev. B* 36 (11) (1987) 6213.
- [36] J. Scholtes, *Fresenius' J. Anal. Chem.* 353 (1995) 499.
- [37] Y. Enta, T. Kinoshita, S. Suzuki, S. Kono, *Phys. Rev. B* 39 (2) (1989) 1125.
- [38] J.E. Ortega, R. Miranda, *Appl. Surf. Sci.* 56–58 (1992) 211.
- [39] M.L. Yu, N.D. Lang, *Phys. Rev. Lett.* 50 (2) (1983) 127.
- [40] M.L. Yu, *Phys. Rev. B* 29 (4) (1984) 2311.
- [41] S.Y. Davydov, A.V. Pavlyk, *Tech. Phys.* 49 (2004) 1050.
- [42] T. Maeda Wong, D. Heskett, N.J. DiNardo, E.W. Plummer, *Surf. Sci. Lett.* 208 (1989) L1.